

# Interpretation of the temperature dependence of $\text{Mn}^{2+}$ high-field ESR spectra in the first incommensurately modulated phase of betaine calcium chloride dihydrate

H. Metz

*Fakultät für Physik und Geowissenschaften, Universität Leipzig, Linnéstrasse 5, D-04103 Leipzig, Germany*

R. Heidler

*Schlumberger, 110 Gillingham Lane, Stafford, Texas 77478*

D. Michel

*Fakultät für Physik und Geowissenschaften, Universität Leipzig, Linnéstrasse 5, D-04103 Leipzig, Germany*

W. Windsch

*Mühlengrund 36, D-04703 Polkenberg, Germany*

(Received 15 September 1997)

By a combination of  $X$ -band and  $Q$ -band ESR investigations it was possible to distinguish between effects of first and second order in the critical behavior, which are influenced in different ways by the dynamics of the order-parameter fluctuations. The theoretical analysis is based on a Fourier expansion of the ESR fine-structure elements in terms of the harmonics of the incommensurate modulation. Second-order perturbation theory for the evaluation of the ESR spectra was applied. The splitting between the edge singularities should show a temperature dependence given by the superposition of two different critical contributions:  $\Delta B_{\text{ES}} = a(T_i - T)^\beta + b(T_i - T)^{2\beta}$ . The second contribution depends on the strength of the external magnetic field. This could be clearly revealed in the comparison between  $Q$ - and  $X$ -band measurements. The influence of the Mn content  $c_{\text{Mn}}$  or of the  $\gamma$ -irradiation dose  $c_\gamma$  on the splitting of the edge singularities was analyzed. [S0163-1829(98)03929-0]

## I. INTRODUCTION

Betaine calcium chloride dihydrate, BCCD,  $(\text{CH}_3)_3\text{N}^+\text{CH}_2\text{COO}^-\text{CaCl}_2 \cdot 2\text{H}_2\text{O}$  belongs to the well-known family of ferroelectric compounds formed by an alpha-amino acid and an inorganic adduct, like for instance trissarcosine calcium chloride and triglycine sulphate.<sup>1</sup> The main interest in this substance lies in the rich variety of commensurately and incommensurately (IC) modulated phases which BCCD exhibits below 164 K.<sup>2</sup>

It is well known that the properties of IC systems may be very sensitively influenced by the incorporation of defects.<sup>3</sup> Small amounts of defects shift the N-IC phase temperature  $T_i$  of the normal (N) to the incommensurate phase and suppress narrow commensurate and incommensurate phases. For the present system  $\text{Mn}^{2+}$  ions are very suitable probes. On the one hand they appear as natural impurities in many Ca compounds as well as in BCCD at Ca sites. Furthermore,  $\text{Mn}^{2+}$  ions prove to be appropriate and sensitive ESR probes. On the basis of our previous papers in which ESR line-shape investigations of  $\text{Mn}^{2+}$  ions in BCCD in its first incommensurately modulated phase were reported, the paramagnetic properties of the system BCCD: $\text{Mn}^{2+}$  are rather well understood.<sup>4,5</sup>  $\text{Mn}^{2+}$  substitutes  $\text{Ca}^{2+}$  and is therefore surrounded by two Cl atoms, two oxygens of the crystal water and two oxygens of the carboxyl groups of the betaines. In the normal phase the  $\text{Ca}^{2+}$  ions and therefore also the  $\text{Mn}^{2+}$  ions are located in the (010)-mirror planes at  $y = 1/4$  and  $3/4$ . The observed ESR-spectra are characterized by a large fine-

structure splitting of  $D/g\beta = (958.5 \pm 0.5)$  G and  $E/g\beta = (32 \pm 2)$  G. In accordance with the symmetry of the  $\text{Mn}^{2+}$  site, the principal axes  $Y_m$  and  $Z_m$  of the fine-structure tensor lie in the (010)-mirror plane, with an angle of  $51^\circ$  between the  $Z_m$  direction and the crystallographic  $c$  axis. The magnetic  $X_m$  axis is parallel to the crystallographic  $b$  axis.

In the first incommensurately modulated phase one obtains the typical line shape with edge singularities. In the previous papers a model was developed to interpret the observed line shape on the basis of the assumption of two tiltings of the fine-structure tensor, both of which are coupled with the incommensurate modulation wave.<sup>4,6</sup> One of these rotations (angle  $\Delta\Psi$ ) occurs around the magnetic  $Z_m$  axis and the other one around the magnetic  $Y_m$  axis (angle  $\Delta\Phi$ ). If these tiltings are coupled directly to the order parameter one expects that the temperature dependence of the amplitude behaves like the order-parameter amplitude  $\eta \propto (T_i - T)^\beta$  with the critical exponent  $\beta = 0.35$  as it was investigated in detail by NMR spectroscopy<sup>11,15,16</sup> and which is consistent with x-ray diffraction studies.<sup>5,7</sup> Our previous ESR measurements showed that this behavior is found only for the tilting  $\Delta\Psi$  about the magnetic  $Z_m$  axis.<sup>4</sup> In contrast, the tilting  $\Delta\Phi$  about the magnetic  $Y_m$  axis showed a temperature dependence according to  $\Delta\Phi \propto (T_i - T)^\gamma$  with an exponent  $\gamma$  which depends on the concentration of the defects and which does not seem to be of physical significance. In this context it has to be mentioned that in the previous measurements at 9.4 GHz, the treatment of the spectra required an exact diagonalization of the spin Hamiltonian due to the very large

fine-structure interaction and, thus, led to a rather intricate explanation of the ESR line shape in the IC phase. Therefore, in order to overcome possible problems in the previous investigations, ESR measurements in the  $Q$  band (34 GHz) were performed.<sup>6</sup> In contrast to the  $X$  band, under these conditions the second-order perturbation theory for the analysis of the spin Hamiltonian is sufficient to describe the spectra in the high-temperature phase. On this basis also, the line shape in the first IC phase may be explained unambiguously.

In principle, the line shape in the IC phase depends on all tensor elements of the fine-structure tensor. In particular, the number of relevant parameters that describe the ESR spectra in the  $Q$  band will be smaller and the connection between the tensor elements  $D_{ij}$  and the line shape and line splitting becomes more clear and definite, if the measurements are performed in a particularly selected orientation. A derivation of the final equations to describe the line-shape behavior in the IC phase will be given in Sec. III. On this basis, a reinterpretation and extension of our previous paper will be possible.

In addition to the study of the effect of the Mn concentration on the phase transition the influence of  $\gamma$  irradiation on the  $\text{Mn}^{2+}$ -ESR spectra has been investigated starting from the known fact that one of the defects created by the irradiation is the  $\dot{\text{N}}(\text{CH}_3)_3$  radical, which was already investigated by the ESR and electron-nuclear double resonance (ENDOR) methods.<sup>8-10</sup>

## II. EXPERIMENT

The  $\text{BCCD}:\text{Mn}^{2+}$  single crystals were grown by slow evaporation of a saturated aqueous solution. In order to obtain the required concentration of  $\text{Mn}^{2+}$  ions different amounts of  $\text{MnCl}_2$  were added to this solution. The crystals grown possess concentrations of  $\text{Mn}^{2+}$  within the range of 0.01–up to 5 mol %. For the investigation of the influence of the  $\gamma$ -irradiation defects,  $\text{BCCD}:\text{Mn}^{2+}$  crystals were used with a content of 0.1 mol % Mn and with an additional  $\gamma$  irradiation by a dose of 0.1, 0.3, 0.5, and 1.0 Mrad.

In order to investigate the influence of the IC modulation on the fine-structure tensor versus the temperature close to  $T_i$ , two different types of measurements were run. In the  $X$  band the ESR line shape of the  $5/2 \rightleftharpoons 3/2$  fine-structure transition was measured for an orientation of the magnetic field  $B_0$  along the magnetic axis  $Z_m$ . The  $-5/2 \rightleftharpoons -3/2$  fine-structure transition for the orientation of the magnetic field  $B_0$  along the magnetic axis  $Z_m$  was chosen for the studies in the  $Q$  band. The ESR measurements were carried out by means of a Varian E112 spectrometer ( $X$  band) and a Bruker ESP 380 spectrometer ( $Q$  band) with a nitrogen flow cryostat to control the temperature.

## III. THEORY

All further calculations will be referred to a laboratory frame (LF) of coordinates  $(x, y, z)$  (Fig. 1) with  $z$  parallel to the external magnetic field  $B_0$ , which is identical with the directions of the principal axes  $(X_m, Y_m, Z_m)$  of the  $\text{Mn}^{2+}$  fine-structure tensor in the high-temperature normal phase (N). This is achieved by a suitable crystal orientation.

The derivation of the final equations for the line shape is

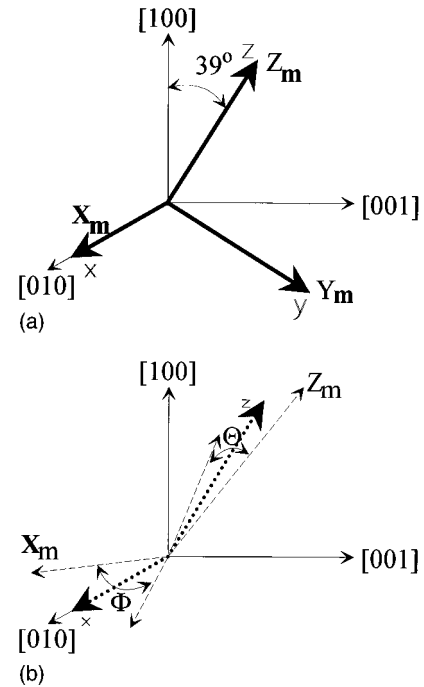


FIG. 1. (a) Orientation of the magnetic axes system  $(X_m, Y_m, Z_m)$  and the position of the laboratory axes system (LF)  $(x, y, z)$  in the crystallographic axes system  $(a, b, c)$ . (b) Orientation of the magnetic axes system  $(X_m, Y_m, Z_m)$  in the incommensurate phase.

similar to the results given by Walisch *et al.*<sup>11</sup> for the quadrupolar perturbed  $^{87}\text{Rb}$  NMR measurements of  $\text{Rb}_2\text{ZnCl}_4$ . Extending the treatment in which Walisch *et al.* developed a perturbation theory for the quadrupolar Hamiltonian in first order, in the present case second-order effects on the fine-structure Hamiltonian have to be considered in the calculation of the ESR spectra.

The line-shape analysis is based on the Fourier expansion of the fine-structure interaction, which is responsible for the ESR line shape in the IC phase of the system  $\text{BCCD}:\text{Mn}^{2+}$ . To select the main contributions in this series it will be necessary to take into account the symmetry properties in the normal (N) and the commensurate ferroelectric (C) low-temperature phase, i.e., to take advantage of the superspace symmetry. According to the symmetry analysis it has been found that the IC modulation is connected with a tilt of the fine-structure axis  $Z_m$  out of this (010) plane in the direction of the  $[010]$  axis, i.e., a rotation by an angle  $\theta$  around the  $y$  axis of the LF. Note again that  $Z_m$  lies in the (010) plane in case of the normal phase [see Fig. 1(a)]. Hence, in relation to the laboratory frame chosen [Fig. 1(b)] also the off-diagonal tensor element  $D_{xz}$  will play an important role in the line-shape calculation for the IC phase.

Taking into account the Zeeman term and the fine-structure interaction, the spin Hamiltonian takes the form

$$\hat{H} = g\beta B_0 \hat{S}_z + \hat{S} D \hat{S} = g\beta B_0 S_z + D_{xx} S_x^2 + D_{yy} S_y^2 + D_{zz} S_z^2 + D_{xz} (S_x S_z + S_z S_x)$$

in the LF  $(x, y, z)$  defined above [Fig. 1(b)].<sup>12</sup> The tensor elements are  $D_{xx} = 1/3D(2 - 3 \cos^2 \theta) + E \cos^2 \theta$ ,  $D_{yy} = -1/3D - E$ ,  $D_{zz} = 1/3D(2 - 3 \sin^2 \theta) + E \sin^2 \theta$ ,  $D_{xz} = (D - E) \sin$

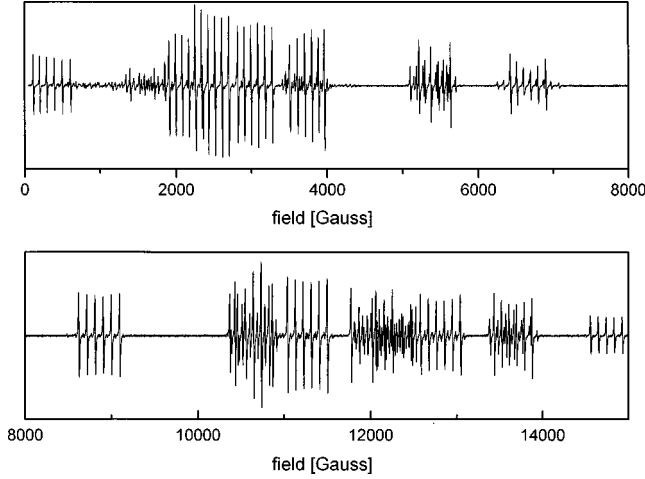


FIG. 2. ESR spectra in the X and Q band at room temperature, rotation around [010],  $B_0 \parallel Z_{m1} - 25^\circ$  and  $B_0 \parallel [100] + 14^\circ$ , superposition of both sites.

$\theta \cos \theta$ , which are simply related with the fine-structure principal axis frame ( $D_{XX} = 1/3D - E$ ,  $D_{YY} = 1/3D + E$ ,  $D_{ZZ} = -2/3D$ ) by a rotation around the  $y$  axis with an angle  $\theta$  as already mentioned.  $\theta$  is the angle between the  $Z_m$  axis and the direction of the external magnetic field  $B_0$  (see Fig. 2).

In the following the treatment is confined to the  $5/2 \rightleftharpoons 3/2$  fine-structure transition with an orientation of the magnetic field  $B_0$  along the magnetic  $z$  axis ( $B_0 \parallel z$ ) in the X band and to the  $-5/2 \rightleftharpoons -3/2$  fine-structure transition in the Q band with the same orientation of the magnetic field  $B_0$ . This simplifies the equations and their discussion. In addition, we may neglect the rhombic contribution of the fine-structure tensor as the  $E$  value is small and consider only the case of axial symmetry.

With  $Bg\beta = \Delta\nu h$  for these transitions we arrive at<sup>12-14</sup>

$$B = B_0 \pm 2D/(g\beta)(3 \cos^2 \theta - 1) + 1/(B_0 g^2 \beta^2)[D^2 \sin^4 \theta - 32/(B_0 g^2 \beta^2)[D^2 \sin^2 \theta \cos^2 \theta]]. \quad (1)$$

The third term  $1/(B_0 g\beta)[D^2 \sin^4 \theta]$  can be neglected if the angle  $\theta$  is small. In BCCD this term is two orders of magnitude smaller than the fourth term since for  $B_0 \parallel z$  the polar angle is  $\theta < 6^\circ$ . Thus, we can rewrite Eq. (1) as

$$B = B_0 \pm 6D_{zz}/(g\beta) - 32D_{xz}^2/(g^2 \beta^2 B_0). \quad (2)$$

According to the treatment by Petersson *et al.*<sup>11</sup> each tensor element is expanded in a Fourier series

$$D_{ij} = D_{ijN} + \sum D_{ijn} \cos(nv + \varphi_n)$$

with the inner variable  $v$  ( $0 \leq v \leq 2\pi$ ) and the tensor elements  $D_{ijN}$  for the normal phase.<sup>11</sup>

As discussed above only two tensor elements  $D_{zz}$  and  $D_{xz}$  are relevant in the first IC phase for BCCD:Mn<sup>2+</sup> because of the symmetry of the N phase and the chosen  $B_0$  orientation. They depend in the following way on the inner variable  $v$  if only the lowest term in the Fourier series is taken into account:

$$D_{zz} = D_{zzN} + D_{zz2} \cos(2v + \varphi_2), \quad (3)$$

$$D_{xz} = D_{xz1} \cos(v + \varphi_1). \quad (4)$$

In Eq. (3) a term  $D_{zz1}$  is forbidden because of symmetry.  $D_{xzN}$  is identical to zero in the normal phase (N). As shown in Ref. 11 the parameters  $D_{xz1}$  and  $D_{zz2}$  show a critical temperature dependence below  $T_i$  according to the power laws

$$D_{zz2} \propto (T_i - T)^{\bar{\beta}}, \quad (5)$$

$$D_{xz1} \propto (T_i - T)^\beta, \quad (6)$$

where  $\bar{\beta}$  is different from  $2\beta$ .<sup>11</sup> Within the 3d-XY model which was found to be applicable to the description of the N-IC phase transition the values for these critical exponents are expected to be<sup>15,16,18</sup>

$$\beta \approx 0.34,$$

$$\bar{\beta} \approx 0.83.$$

Substitution of Eqs. (3) and (4) into Eq. (2) leads to the formula

$$B = B_0 \pm 6D_{zzN}/(g\beta) + B(v) \quad (7)$$

with the function

$$B(v) = \pm 6D_{zz2} \cos(2v + \varphi_2)/(g\beta) - 32[D_{xz1} \cos(v + \varphi_1)]^2/(B_0 g^2 \beta^2).$$

The position of the edge singularities can be calculated according to the condition  $\delta B(v)/\delta v = 0$ .

The midpoint (MP) between the edge singularities (ES) can be calculated by an averaging about the inner variable  $v$  in Eq. (7) and provides

$$B_{MP} = B_0 \pm 6D_{zzN}/(g\beta) - 16/(B_0 g^2 \beta^2)[D_{xz1}]^2. \quad (8)$$

This position of the MP only depends on the parameter  $D_{xz1}$  and is independent of the phase factors  $\varphi_1$  and  $\varphi_2$ . Equation (8) in combination with Eq. (6) shows that the MP behaves like the square of the order-parameter amplitude.

On the other hand, no analytic expression exists for the splitting between the edge singularities  $\Delta B_{ES}$ , if no assumption for the phases  $\varphi_1, \varphi_2$  is made. In the case of  $\varphi_1 = \varphi_2$  the distance between the edge singularities can be described as follows:

$$\Delta B_{ES} = 3D_{zz2}/(g\beta) - 16/(B_0 g^2 \beta^2)[D_{xz1}]^2. \quad (9)$$

With Eqs. (5) and (6) the splitting between the edge singularities should show a temperature dependence given by the superposition of two different critical contributions

$$\Delta B_{ES} = a(T_i - T)^{\bar{\beta}} + b(T_i - T)^{2\beta}. \quad (10)$$

In a previous paper<sup>6</sup> we tried to explain the ES splitting by an equation like

$$\Delta B_{ES} = c(T_i - T)^\gamma \quad (11)$$

because we found in the plots of  $\ln(\Delta B_{ES})$  versus  $(T_i - T)$  nice straight lines.

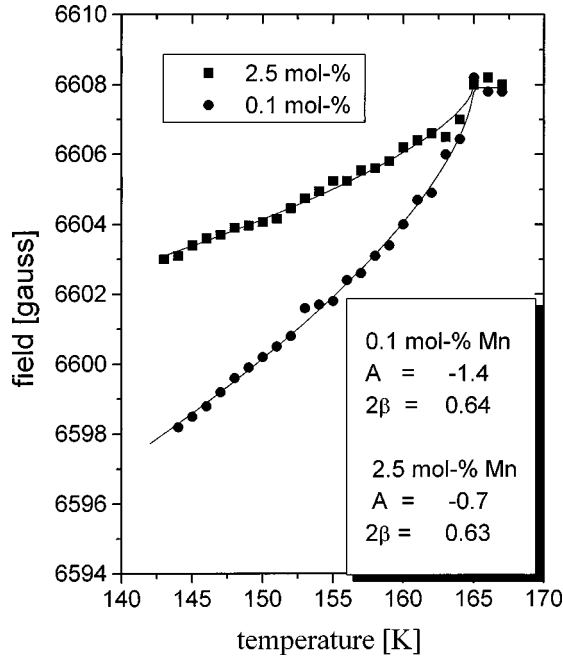


FIG. 3. Temperature dependence of the midpoint between the edge singularities in the  $X$  band and the fit curves for the manganese concentrations 2.5 and 0.1 mol %.

Hence we expect from Eq. (10) an effective critical exponent  $\gamma$  in the range between  $2\beta \approx 0.68$  and  $\bar{\beta} \approx 0.83$  if both prefactors are positive, i.e.,  $a, b > 0$ . In the case  $a > 0$  and  $b < 0$  the first term in Eq. (10) increases the splitting between the edge singularities if it dominates and the second term tries to decrease the splitting or vice versa if the second term in Eq. (10) dominates. Both cases are possible since the second term in Eq. (10) depends on the external magnetic field. As a consequence we expect a different behavior in the  $X$  band and in the  $Q$  band.

Now we must establish under which assumptions we can expect that the splitting between the edge singularities give a straight line in the semilog plots or when we approximate Eq. (10) by Eq. (11),  $[a(T_i - T)^\beta + b(T_i - T)^{2\beta} \approx c(T_i - T)^\gamma]$ . This problem was investigated on the basis of simulations. We have obtained the following results, which are independent of the phase factors in Eq. (7):

(1) A function  $a(T_i - T)^\beta + b(T_i - T)^{2\beta}$ , with  $a > 0$  and  $b < 0$ , can be analyzed by a function  $c(T_i - T)^\gamma$  in a temperature range of about 10 K below  $T_i$  if the ratio of the prefactors of the power laws ( $-a/b$ ) [Eqs. (5) and (6)] or  $|a/b|$  lies in the range from 2.0 to 4.9.

(2) The effective exponent  $\gamma$  lies then in the range  $\gamma < 2\beta$  which corresponds to the experimentally observed values of these exponents (see Sec. IV).

#### IV. ANALYSIS OF THE EXPERIMENTAL RESULTS

##### A. Temperature dependence of the midpoint between the edge singularities in the $Q$ band and $X$ band

The experimental  $Q$ -band results for two different  $\text{Mn}^{2+}$  concentrations (0.1, 2.5 mol %) are shown in Fig. 3. The influence of the manganese concentration is clearly visible. In Eq. (8) it was assumed that  $D_{zzN}$  is temperature

TABLE I. Fit results according to Eq. (12) of the temperature-dependent ESR measurements in the  $Q$  band for BCCD with different  $\text{Mn}^{2+}$  concentrations.

$\text{Mn}^{2+}$ concentration $c_{\text{Mn}}$ (mol %)	$A_1$ (G/K)	$T_i$ (K)	$2\beta$	$A_2$ (G/K)
0.01	2.2	164.8	0.67	-0.5
0.1	1.9	164.4	0.74	-0.5
2.5	1.7	163.6	0.69	-0.3
Error	$\pm 0.2$	$\pm 0.1$	$\pm 0.08$	$\pm 0.2$

independent which is not valid in our experiments. In the high-temperature phase (N) we have a strong, nearly linear shift of the resonance position of the ESR lines. We assumed that the same linear variation occurs also in the IC phase and added in Eq. (8) an additional term  $A_2(T_i - T)$ . Hence, we fitted the position of the MP with the function

$$B_{\text{MP}} = D_0(T_i) + A_1(T_i - T)^{2\beta} - A_2(T_i - T), \quad (12)$$

$$D_0(T_i) = B_0 \pm 6D_{zzN}(T_i)/g\beta = \text{const.}$$

The results of the fits are summarized in Table I.

It should be taken into account that the constant term  $D_0(T_i) = B_0 + 6D_{zzN}(T_i)$  may vary from sample to sample in particular for measurements in the  $Q$  band because of slightly different probe shapes and probe sizes leading to slightly different  $Q$ -band ESR frequencies. Furthermore, the linear shifts in the  $Q$ -band ESR spectra mentioned above are not very large and give rise to small additional errors to the fit parameter. Nevertheless, the critical exponent  $\beta$  can be estimated rather precisely to be  $\beta = 0.34 \pm 0.04$ .

The  $X$ -band data were analyzed in the same manner although the second-order perturbation theory is not sufficient. The results of the fits are given in Table II. Despite the inaccuracy of Eq. (8) for the  $X$  band (see below) due to the greater shifts in the  $X$ -band spectra and therefore the greater precision in determining the midpoint between the edge singularities, the errors lie in the same range.

##### B. Temperature dependence of the splitting between the edge singularities in the $Q$ band and $X$ band

The splitting of the edge singularities  $\Delta B_{\text{ES}}$  is independent of the temperature dependence of  $D_{zzN}$  and was analyzed using Eqs. (10) and (11). The results of the fits are given in Table III. The prefactors  $a$  and  $b$  [Eq. (10)] and  $c$  [Eq. (11)] decrease drastically with increasing  $\text{Mn}^{2+}$  content. In Fig. 4 the experimental data for the  $X$  band are shown.

TABLE II. Fit results according to Eq. (12) of the temperature-dependent ESR measurements in the  $X$  band for BCCD with different  $\text{Mn}^{2+}$  concentrations.

$\text{Mn}^{2+}$ concentration $c_{\text{Mn}}$ (mol %)	$A_1$ (G/K)	$2\beta$	$A_2$ (G/K)
0.01	-1.4	0.64	0.3
2.5	-0.7	0.63	0.4
Error	$\pm 0.2$	$\pm 0.06$	$\pm 0.2$

TABLE III. Fit results of the temperature-dependent ESR measurements in the  $Q$  band for BCCD with different  $\text{Mn}^{2+}$  concentrations.

$\text{Mn}^{2+}$ concentration $c_{\text{Mn}}$ (mol %)	$a$	$b$	$-a/b$	$a+b$	$T_i$ (K)	$c$	$\gamma$
0.01	20.3	-9.84	2.06	11.2	164.88	18.3	0.32
0.1	21.8	-10.0	2.18	11.8	164.59	14.0	0.41
1.0	15.6	-6.69	2.33	8.9	163.67	9.0	0.46
2.5	5.21	-2.04	2.55	3.2	162.31	3.3	0.52
Error	$\pm 0.5$	$\pm 0.5$	$\pm 0.2^a$	$\pm 1.0$	$\pm 0.05$	$\pm 0.5$	$\pm 0.05$

<sup>a</sup>In average.

The results of the data fits are given in Tables III and IV for the  $Q$  band and for the  $X$  band, respectively. For the fits our knowledge about the critical exponents  $\beta$  and  $\bar{\beta}$  was used (see Sec. V), i.e., the exponents were fixed to these values. If the splittings are small and the exponent  $\gamma$  is near to  $2\beta$  a good fit cannot be obtained as is the case of the sample with 5 mol %  $\text{Mn}^{2+}$  for measurements in the  $Q$  band which, consequently, was omitted in Table III.

## V. DISCUSSION

As is well known, the incorporation of paramagnetic defects is a prerequisite for ESR investigations. In order to use these techniques for the study of subtle details on dynamic properties and structural changes near the phase transitions in particular the question has to be answered whether and in which way the mechanism of the phase transition is influenced or distorted by the incorporation of paramagnetic defects and other impurities.<sup>17</sup> BCCD crystals doped with  $\text{Mn}^{2+}$  ions are very suitable in order to estimate the possible influence of defects. For this reason a careful investigation of

the temperature dependence of the order parameter and of the respective critical exponents has been performed.

In a first step it was shown that the structural changes near the phase transition are reflected in the fine-structure splitting of the ESR spectra of the  $\text{Mn}^{2+}$  ions. The analysis and explanation of all effects were possible because of the combination of the  $X$ -band and  $Q$ -band ESR measurements. The value  $\beta \approx 0.34$  found for the order parameter is in complete agreement with the results of extensive NMR investigations and x-ray-diffraction studies.<sup>15,7</sup> In principle, the same structural information is contained in the fine-structure and quadrupolar tensors. In particular, it could be shown that the general formalism of the line-shape calculation as developed in Ref. 15 is also applicable for the IC-modulated ESR spectra. In contrast to the quadrupolar perturbed NMR spectra where only first-order quadrupolar effects had to be considered, in this work second order of the perturbation theory for the spin Hamiltonian was necessary for  $\text{Mn}^{2+}$  sites in BCCD crystals. This analysis relies only on the symmetry analysis for the superspace group and on the symmetry of the order parameter. The results confirm the interpretation of the non-classical critical behavior in the IC phase of BCCD in terms of the universality class of the  $3d XY$  model.<sup>18</sup> Since higher-order effects must be considered in the ESR measurements of  $\text{Mn}^{2+}$ -doped BCCD, contrary to the rather simple situation as could be realized in the NMR measurements, the ESR line splitting is the superposition of two contributions. One of them tries to increase the splitting and the other leads to a decrease of the splitting of the edge singularities. Because of the second-order perturbation theory one of the contributions depends on the external magnetic field. This is the reason why the measurements in the  $Q$  band, in comparison with previous  $X$ -band studies, gave valuable hints for the interpretation of the line shape and line splitting in the IC phase of BCCD.

Furthermore the influence of the Mn content and the  $\gamma$  irradiation (Table V) was analyzed. There is a small influence of the  $\text{Mn}^{2+}$  concentration on the phase-transition temperature  $T_i$  (see Tables I and III). The results are reproducible and out of the range of the error of about  $\pm 0.1$  K in the temperature control for the  $Q$ -band ESR measurements. Although the influence is rather small and, thus, is not of importance for the further discussion of the measurements in the first IC phase of BCCD, it is noted that for increasing defect concentration the subsequent small commensurate phase in BCCD ( $2/7$  phase) is smeared out and can no longer be detected by ESR measurements unless the  $\text{Mn}^{2+}$  concen-

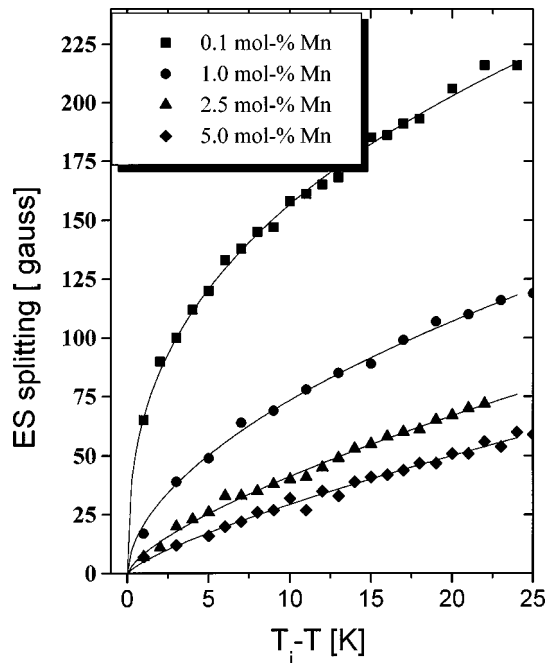


FIG. 4. Temperature dependence of the splitting between the edge singularities in the  $X$  band for the manganese concentrations 0.1, 1.0, 2.5, and 5.0 mol %. Straight lines are the fit results.

TABLE IV. Fit results of the temperature-dependent ESR measurements in the X band for BCCD with different  $\text{Mn}^{2+}$  concentrations.

$\text{Mn}^{2+}$ concentration $c_{\text{Mn}}$ (mol %)	$a$	$b$	$a+b$	$-a/b$	$c$	$\gamma$
0.01	75.6	-30.75	44.9	2.4	66.4	0.31
0.1	49.0	-22.1	26.9	2.2	34.8	0.37
1.0	28.7	-9.1	19.6	3.2	21.0	0.48
2.5	14.5	-3.6	10.9	4.0	8.3	0.58
5.0	9.3	-2.2	7.1	4.2	5.0	0.73
Error	$\pm 0.5$	$\pm 0.5$	$\pm 0.2^a$	$\pm 0.05$	$\pm 0.5$	$\pm 0.05$

<sup>a</sup>In average.

tration is very small (less than about 0.5 mol %). In the further analysis of the influence of the Mn content  $c_{\text{Mn}}$  or the  $\gamma$  dose  $c_\gamma$ , fit parameters  $a$  and  $b$  from the analysis of the spectra in the first IC phase were obtained [Eq. (10)] which are proportional to the square of the order parameter. The graphs in Fig. 5 reveal that the order-parameter amplitude is indirectly proportional to the defect concentration in the investigated Mn concentration and  $\gamma$ -dose ranges. The decrease of the amplitude of the order parameter induced by the defects was also detected by ENDOR investigations on  $\gamma$ -irradiated BCCD at 130 K.<sup>9</sup> Here a decrease of the tilt angle from  $\sim 11^\circ$  to  $\sim 7^\circ$  was determined. The decrease of the order-parameter amplitude detected by ESR for BCCD samples containing 0.1 mol % Mn and, additionally, irradiated with a dose of 1 Mrad, is of the same order of magnitude.

Another question concerns the comparison of our results with the study of the influence of defect by Schaack *et al.*<sup>19</sup> where bromine instead of chlorine atoms was introduced into the crystals of the betaine family. The replacement of bromine (with considerably greater ionic radii) for chlorine atoms in BCCD, where a strong dependence of the phase-transition temperature  $T_i$  on the bromine concentration was found, was explained by a negative hydrostatic pressure or by an increase of the unit-cell dimension because of the bromine ion incorporation.<sup>20,21</sup>

First of all we have to remember that  $\text{Mn}^{2+}$  ions are substituted on  $\text{Ca}^{2+}$  sites and are very suitable paramagnetic sites since their ionic radius is very similar to the ionic radius of the  $\text{Ca}^{2+}$  ions. Hence, drastic effects on the phase diagram can be ruled out in the case of  $\text{Mn}^{2+}$  doping of BCCD crystals. The Mn and  $\gamma$  defects influence the phase-transition

TABLE V. Fit results of the temperature-dependent ESR measurements in the Q band for BCCD with a  $\text{Mn}^{2+}$  concentration of 0.1 mol % and an irradiation with different  $\gamma$  doses  $c_\gamma$ .

Gamma-dose $c_\gamma$ (Mrad)	$a$	$b$	$a+b$	$-a/b$	$c$	$\gamma$
0	49.0	-22.1	26.9	2.2	34.8	0.37
0.1	36.0	-14.1	23.9	2.46	21.3	0.41
0.3	30.5	-14.3	16.2	2.12	18.5	0.44
0.5	30.1	-14.0	16.1	2.44	13.0	0.54
1.0	24.6	-10.2	14.4	3.37	11.3	0.60

temperature  $T_i$  only very little. Therefore we can expect that the other phase transition temperatures are also scarcely affected in case of the present defects and, hence, the phase diagram of BCCD should not be changed although a distinct decrease of the amplitude of the order parameter, i.e., of the amplitude of the modulation wave, with rising defect concentration is clearly seen.

Two phenomenological theories were applied to describe the phase diagram of BCCD, the ANNNI model (axial- or anisotropic-next-nearest-neighbor Ising)<sup>22</sup> and a Landau-type

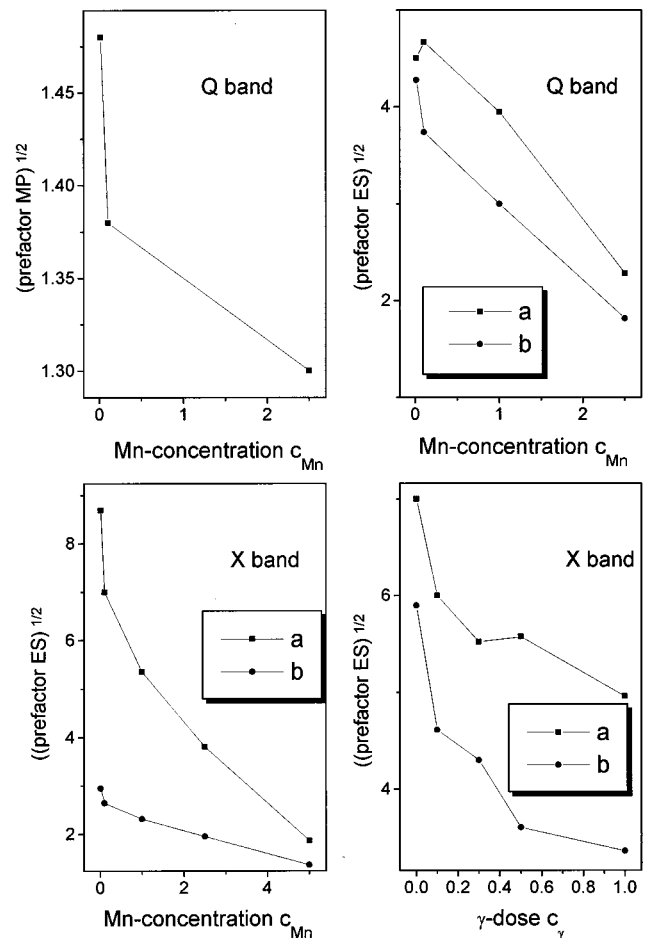


FIG. 5. Dependence of the root of the prefactor  $a$  and the root of the absolute value of the prefactor  $b$  on the  $\gamma$  dose  $c_\gamma$  and on the manganese concentrations  $c_{\text{Mn}}$  in the X band and the Q band. Straight lines are guides for eyes.

model proposed by Sannikov.<sup>23</sup> Both models do not explain the critical behavior of the HT-IC phase transition but can well reproduce the  $p$ - $T$  phase diagram of BCCD. In the framework of the ANNNI model the values and the signs of the couplings  $J_0$  (in the  $x,y$  plane,  $J_0 > 0$ ),  $J_1$  (with the next-neighbor perpendicular to the  $x,y$  plane,  $J_1 > 0$ ), and  $J_2$  (with the next-nearest-neighbor perpendicular to the  $x,y$  plane,  $J_2 < 0$ ) play the dominant role.<sup>22</sup> In this context we must conclude that an increase of the defect concentration should influence both interaction parameters  $J_1$  and  $J_2$  in such a way that the ratio  $J_1/J_2$  is not significantly changed. In the framework of a phenomenological Landau-type model proposed by Sannikov<sup>23</sup> a decreasing amplitude of the order parameter influences the phase diagram also only very weakly. Our experimental situation seems to agree very well with theoretical predictions of recent lattice-dynamic calculations.<sup>24</sup> For second-order phase transitions it has been analytically shown that the static critical exponents are not changed for a low defect concentration, and only a decrease of the amplitude of the order parameter is to be expected.

## VI. CONCLUSIONS

ESR studies on paramagnetic defect sites in solids with incommensurate phases are an appropriate tool for the inves-

tigation of structural changes and the critical behavior at the phase transitions if the contributions of the different harmonics of the incommensurate modulation are taken into account. In this way a critical exponent of the order parameter in the system BCCD:Mn<sup>2+</sup> of  $\beta = 0.34 \pm 0.04$  was determined which is in good agreement with the results of NMR and x-ray measurements on undoped BCCD crystals. For very low (up to  $\sim 0.1$  mol %) Mn<sup>2+</sup> defect concentrations or doses of  $\gamma$  radiation neither the phase-transition temperature and the critical exponent nor the amplitude of the order parameter are changed. At higher defect concentrations (up to  $\sim 2.5$  mol % of Mn<sup>2+</sup> ions and 1 Mrad  $\gamma$  doses) no influence on the critical exponent  $\beta$  could be found and the transition temperature is changed no more than about 1 K. The amplitude of the order parameter, however, varies approximately inversely proportional to the defect concentration. This result is also consistent with recent theoretical work.

## ACKNOWLEDGMENTS

We are indebted to Dr. A. Klöpperpieper and K. Kretsch (Saarbrücken) for growing and characterizing the high-quality crystal samples. Financial support by the Deutsche Forschungsgemeinschaft is gratefully acknowledged.

- <sup>1</sup>W. Brill, W. Schildkamp, and J. Spilker, *Z. Kristallogr.* **172**, 281 (1986).
- <sup>2</sup>A. Klöpperpieper, H. J. Rother, J. Albers, and H. E. Müser, *Jpn. J. Appl. Phys., Part 1* **24**, 829 (1986).
- <sup>3</sup>K. Hamono, in *Incommensurate Phases in Dielectrics*, Vol. 2: *Materials*, edited by R. Blinc and A. P. Levanyuk (North-Holland, Amsterdam, 1986), Chap. 9.
- <sup>4</sup>R. Heidler, H. Metz, and W. Windsch, *Ferroelectrics* **125**, 419 (1992).
- <sup>5</sup>R. Heidler, H. Metz, M. le Maire, G. Schaack, and W. Windsch, *Chem. Phys. Lett.* **209**, 299 (1993).
- <sup>6</sup>R. Heidler, H. Metz, and W. Windsch, *Chem. Phys. Lett.* **229**, 143 (1994).
- <sup>7</sup>W. Brill and K. H. Ehses, *Jpn. J. Appl. Phys., Part 1* **24**, 826 (1988).
- <sup>8</sup>H. Metz and R. Böttcher, *Appl. Magn. Reson.* **9**, 319 (1995); **10**, 603 (1996).
- <sup>9</sup>H. Metz and R. Böttcher, *Appl. Magn. Reson.* **12**, 127 (1997).
- <sup>10</sup>H. Metz, G. Schaack, M. Schmitt, and W. Windsch, *Phys. Status Solidi A* **126**, K73 (1991).
- <sup>11</sup>R. Walisch, J. M. Perez-Mato, and J. Petersson, *Phys. Rev. B* **40**, 10 747 (1989).
- <sup>12</sup>A. Abragam and B. Bleaney, *Electron Paramagnetic Resonance of Transition Ions* (Dover, New York, 1986).
- <sup>13</sup>W. Low, *Paramagnetic Resonance in Solids*, Solid State Physics Suppl. 2, (Academic, New York, 1960).
- <sup>14</sup>G. Schoffa, *Elektronenspinresonanz in der Biologie (bibliotheca biophysica)*, edited by B. Rajewski (Braun, Karlsruhe, 1964).
- <sup>15</sup>K.-P. Holzer, J. Petersson, D. Schüssler, R. Walisch, U. Häcker, and D. Michel, *Phys. Rev. Lett.* **71**, 89 (1993).
- <sup>16</sup>K.-P. Holzer, U. Häcker, J. Petersson, D. Michel, and S. Kluthe, *Solid State Commun.* **94**, 275 (1995).
- <sup>17</sup>K. A. Müller and J. C. Fayet, *Structural Phase Transition Studied by Electron Paramagnetic Resonance in Structural Phase Transition II*, Topics in Current Physics, edited by K. A. Müller and H. Thomas (Springer-Verlag, Berlin, 1990), pp. 1–82.
- <sup>18</sup>A. D. Bruce and R. A. Cowly, *J. Phys. C* **11**, 3609 (1978). A. D. Bruce, R. A. Cowly, and A. F. Murray, *J. Phys. C* **11**, 3591 (1978).
- <sup>19</sup>M. le Maire, A. Lopez Ayala, G. Schaack, A. Klöpperpieper, and H. Metz, *Ferroelectrics* **157**, 355 (1993); G. Schaack, *Acta Phys. Pol. A* **83**, 451 (1993); R. Ao, G. Schaack, M. Schmitt, and M. Zöller, *Phys. Rev. Lett.* **62**, 183 (1989).
- <sup>20</sup>M. LeMaire, A. Lopez Ayala, and G. Schaack, *Ferroelectrics* **155**, 335 (1994).
- <sup>21</sup>G. Schaack, M. LeMaire, M. Schmitt-Leven, M. Illing, A. Lengel, M. Manger, and R. Straub, *Ferroelectrics* **183**, 205 (1996).
- <sup>22</sup>W. Selke, *Phys. Rep.* **170**, 213 (1988).
- <sup>23</sup>D. G. Sannikov, *Ferroelectrics* **124**, 49 (1991); (private communication).
- <sup>24</sup>H. Breater (private communication).